

# Experimental realization of phase-controlled dynamics with hybrid digital-analog approach

**Ziyu Tao**

Southern University of Science and Technology <https://orcid.org/0000-0003-3633-6000>

**Libo Zhang**

Southern University of Science and Technology

**Xiaole Li**

Southern University of Science and Technology

**Jingjing Niu**

Southern University of Science and Technology

**Kai Luo**

Southern University of Science and Technology

**Kangyuan Yi**

Southern University of Science and Technology

**Yuxuan Zhou**

Southern University of Science and Technology

**Hao Jia**

Southern University of Science and Technology

**Song Liu**

Institute for Quantum Science and Engineering and Department of Physics, South University of Science and Technology of China

**Tongxing Yan** (✉ [yantx@sustech.edu.cn](mailto:yantx@sustech.edu.cn))

Southern University of Science and Technology

**Yuanzhen Chen**

Southern University of Science and Technology

**Da-Peng Yu**

Southern University of Science and Technology

---

## Article

**Keywords:** chiral dynamics, closed-contour interaction, quantum simulation

**Posted Date:** August 17th, 2020

**DOI:** <https://doi.org/10.21203/rs.3.rs-50234/v1>

**License:**  This work is licensed under a Creative Commons Attribution 4.0 International License.

[Read Full License](#)

---

**Version of Record:** A version of this preprint was published at npj Quantum Information on May 18th, 2021. See the published version at <https://doi.org/10.1038/s41534-021-00406-1>.

# Experimental realization of phase-controlled dynamics with hybrid digital-analog approach

Ziyu Tao,<sup>1,2,3,\*</sup> Libo Zhang,<sup>1,2,3,\*</sup> Xiaole Li,<sup>1,2,3</sup> Jingjing Niu,<sup>1,2,3</sup> Kai Luo,<sup>1,2,3</sup> Kangyuan Yi,<sup>1,2,3</sup>  
Yuxuan Zhou,<sup>1,2,3</sup> Hao Jia,<sup>1,2,3</sup> Song Liu,<sup>1,2,3,†</sup> Tongxing Yan,<sup>1,2,3,‡</sup> Yuanzhen Chen,<sup>1,2,3,§</sup> and Dapeng Yu<sup>1,2,3</sup>

<sup>1</sup>*Shenzhen Institute for Quantum Science and Engineering and Department of Physics,  
Southern University of Science and Technology, Shenzhen 518055, China*

<sup>2</sup>*Guangdong Provincial Key Laboratory of Quantum Science and Engineering,  
Southern University of Science and Technology, Shenzhen, 518055, China*

<sup>3</sup>*Shenzhen Key Laboratory of Quantum Science and Engineering,  
Southern University of Science and Technology, Shenzhen 518055, China*

(Dated: July 28, 2020)

Quantum simulation can be implemented in pure digital or analog ways, each with their pros and cons. By taking advantage of the universality of a digital route and the efficiency of analog simulation, hybrid digital-analog approaches can enrich the possibilities for quantum simulation. We use a unique hybrid approach to experimentally perform a quantum simulation of phase-controlled dynamics resulting from a closed-contour interaction (CCI) within certain multi-level systems in superconducting quantum circuits. Due to symmetry constraints, such systems cannot host an inherent CCI. Nevertheless, by assembling analog modules corresponding to their natural evolutions and specially designed digital modules constructed from standard quantum logic gates, we can bypass such constraints and realize an effective CCI in these systems. Based on this realization, we demonstrate a variety of related and interesting phenomena, including phase-controlled chiral dynamics, separation of chiral enantiomers, and a new mechanism to generate entangled states based on CCI.

Digital quantum simulation relies on decomposition of the evolution of a targeted Hamiltonian into a sequence of discrete quantum logic gates.<sup>1-3</sup> While in principle this can be done for an arbitrary quantum system,<sup>4</sup> it often requires an intimidating number of gate operations with high precision. Analog approaches exploiting the continuous nature of quantum evolutions may often be more efficient,<sup>5-8</sup> but usually must be designed on an *ad hoc* basis. Hybrid digital-analog quantum simulation has thus been proposed to combine the universality of digital approaches with analog efficiency.<sup>9-12</sup> The flexibility in engineering and assembling digital and analog modules generates abundant possibilities for quantum simulation that are hardly available otherwise. For example, in a simulation of the quantum Rabi model,<sup>13</sup> a deep-strong coupling that is inaccessible to pure analog or digital approaches could be realized via a hybrid method.<sup>14</sup>

In this work, we show that by employing a hybrid method, one can perform quantum simulations that otherwise cannot be implemented on a given platform. In particular, we demonstrate phase-controlled quantum dynamics and related phenomena via closed-contour interaction (CCI) in superconducting quantum circuits, which was originally forbidden by certain symmetry-imposed selection rules. The simplest realization of CCI involves a three-level system. Such systems with two of the three possible transitions being coherently driven have been widely researched for both fundamental interest and promising applications in areas such as quantum sensing<sup>15,16</sup> and quantum information processing.<sup>17</sup> By opening the third transition, the three levels form a loop with a CCI, which leads to fundamentally new quantum

phenomena, including phase-dependent coherent population trapping,<sup>18</sup> phase-controlled dynamics,<sup>19</sup> and coherence protection.<sup>20</sup> A closed-loop configuration can also be used in the detection and separation of enantiomers,<sup>21-23</sup> i.e., chiral molecules with left (*L*) and right (*R*) handedness, which has long been a challenging problem in chemistry.<sup>24</sup>

In practice, the implementation of CCI is often hindered by selection rules for transitions imposed by symmetry constraints in realistic systems. Common practice in overcoming this problem includes the simultaneous use of multiple drivings of different types (e.g., both electric and magnetic dipole transitions)<sup>20</sup> or high-order processes such as a two-photon transition.<sup>25,26</sup> Here, we first show that in a three-level system subject to such selection rules, one can engineer the system Hamiltonian by assembling two digital and one analog module to induce a CCI with only two coherent drivings of the same type. Phenomena related to CCI, such as phase-controlled chiral dynamics, are observed. By making such driving fields time-dependent, we are able to demonstrate a proposed scheme to separate chiral molecules with high fidelity,<sup>27</sup> and we can extend our technique to more complex systems. Specifically, we propose and realize a new scheme to generate entangled states using a CCI across two coupled superconducting qubits.

## Results

**Realization of CCI.** Consider a three-level system composed of three states  $\{|g\rangle, |e\rangle, |f\rangle\}$ . The system is coherently driven by two external fields of the same type, such as electric-dipole allowed transitions, that correspond to

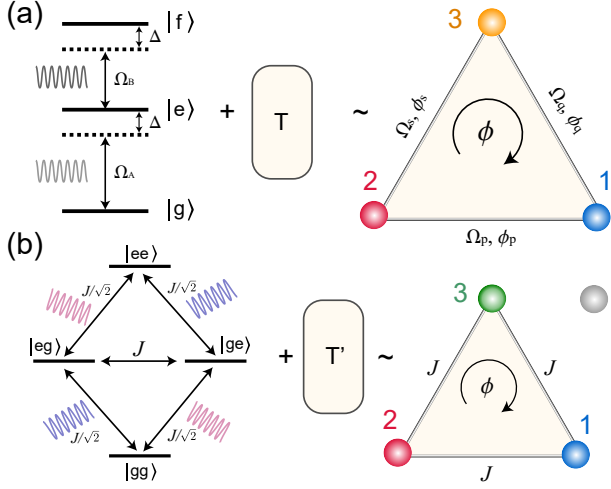


FIG. 1. Realization of CCI with a hybrid digital-analog approach. (a) A three-level system (a qutrit) driven by two detuned external fields (described by a Hamiltonian of  $H_0$ ), when combined with specially designed digital modules (the  $T$  block) constructed from discrete quantum gates, can be used to realize a new Hamiltonian  $H$  hosting an inherent CCI:  $T e^{-iH_0 t} T^\dagger \equiv e^{-iHt}$ , with a gauge-invariant phase  $\phi$ . For consistency with the literature, we relabel the states of the qutrit as  $|g\rangle, |e\rangle, |f\rangle = 1, 2, 3$ . (b) In a similar way, combining the natural evolution of two resonant qutrits driven by two external fields (with identical amplitudes and phases, indicated by different colors) with certain digital modules can result in a CCI in a subspace of the system. Here 1, 2, and 3 correspond to  $|gg\rangle, |ge\rangle$ , and  $|eg\rangle$ , respectively. The gray sphere beside the state of 3 represents a dark state that is decoupled from the evolution of the system (see Methods).

75  $|g\rangle \leftrightarrow |e\rangle$  and  $|e\rangle \leftrightarrow |f\rangle$ . The effective Hamiltonian of the  
76 system under rotating-wave approximation is given by

$$H_0 = \frac{\hbar}{2} \begin{pmatrix} -\Delta_A & \Omega_A^* & 0 \\ \Omega_A & 0 & \Omega_B^* \\ 0 & \Omega_B & \Delta_B \end{pmatrix}, \quad (1)$$

77 where  $\Omega_{A,B}$  and  $\Delta_{A,B}$  are the amplitudes and detunings,  
78 respectively, of the two external driving fields (see Fig.  
79 1(a)).

80 If the system assumes a restrictive symmetry, then the  
81 third transition  $|g\rangle \leftrightarrow |f\rangle$  of the same type is forbid-  
82 den. Even in systems of less restrictive symmetry (e.g.,  
83 artificial atoms such as superconducting qubits), the am-  
84 plitude of such transitions is usually vanishingly small.<sup>28</sup>  
85 Previously, a third driving of a different type or of the  
86 same type but of higher order was used to close the loop  
87 to form a CCI.<sup>25,26</sup> We take a different approach. By  
88 combining an analog module corresponding to the evo-  
89 lution driven by  $H_0$  with two digital modules that are  
90 unitary operators constructed from standard quantum  
91 gates, we effectively transform the original Hamiltonian

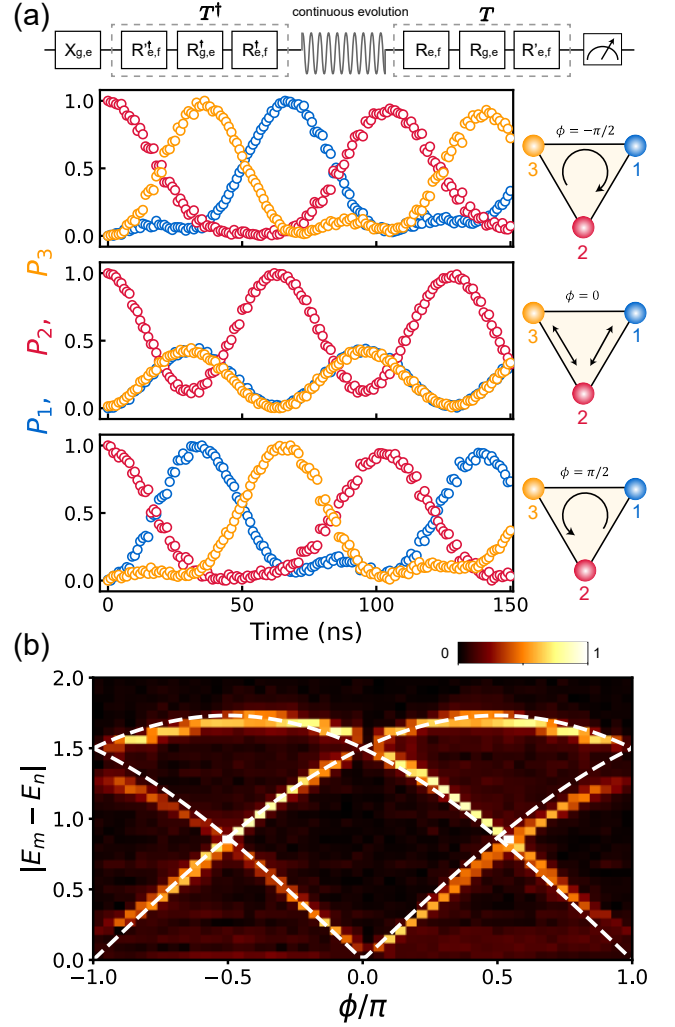


FIG. 2. Phase-controlled quantum dynamics resulting from  
CCI in a single qutrit (see Fig. 1(a)). (a) Upper part:  
flowchart of the experiment, including a block for initializa-  
tion ( $X_{g,e}$ ), a digital module of  $T^\dagger$  composed of three gate  
operations, an analog module of the natural evolution driven  
by  $H_0$ , and another digital module  $T$ , followed by projection  
measurements that yield the three populations of  $P_{1,2,3}$ . Lower  
part:  $P_{1,2,3}$  as functions of the timespan of the intermediate  
natural evolution for three values of the gauge-invariant pa-  
rameter  $\phi$ . (b) Energy spectrum of the Hamiltonian of  $H$  in  
Eq. (2), obtained via discrete Fourier transform of the mea-  
sured populations. It is shown in the form of  $|E_m - E_n|$ , where  
 $E_k$  are the eigenenergies of  $H$ , and  $m, n \in \{1, 2, 3\}$ . Dashed  
white lines represent theoretical predictions.

92  $H_0$  to the following form (see Methods for details):

$$H = \frac{\hbar}{2} \begin{pmatrix} 0 & \Omega_p e^{-i\phi_p} & \Omega_q e^{i\phi_q} \\ \Omega_p e^{i\phi_p} & 0 & \Omega_s e^{-i\phi_s} \\ \Omega_q e^{-i\phi_q} & \Omega_s e^{i\phi_s} & 0 \end{pmatrix}. \quad (2)$$

93 To arrive at the above form, we set the am-  
94 plitudes and detunings of the two drivings  
95 to  $\Omega_A = [\Omega_p e^{i\phi_p} + \Omega_s e^{i(\phi_q - \phi_s)}] / \sqrt{2}$ ,  $\Omega_B =$

96  $[-\Omega_p e^{i(\phi_q - \phi_p)} + \Omega_s e^{i\phi_s}] / \sqrt{2}$ , and  $\Delta_{A,B} = -\Omega_q$ .

97 This new Hamiltonian differs from  $H_0$  in that it nat-  
 98 urally contains nonzero amplitudes for all three possi-  
 99 ble transitions, and the magnitudes and phases of al-  
 100 l three amplitudes can be adjusted independently (see  
 101 Fig. 1(a)). Therefore, inherent CCI dynamics can be  
 102 expected for such a Hamiltonian. In the case of equal  
 103 and constant magnitudes,  $\Omega_{p,q,s} \equiv \Omega$ , the population dyn-  
 104 amics are strongly dependent on the phases  $\phi_{p,s,q}$  of  
 105 the driving fields, through a gauge-invariant global phase  
 106  $\phi = \phi_p + \phi_s - \phi_q$ . We will show an experimental demon-  
 107 stration of such CCI dynamics.

108 We used Xmon-type superconducting qutrits in our  
 109 experimental work. In this kind of artificial atom, the  
 110 transitions of  $|g\rangle \leftrightarrow |e\rangle$  and  $|e\rangle \leftrightarrow |f\rangle$  are electric-dipole  
 111 allowed, whereas the transition  $|g\rangle \leftrightarrow |f\rangle$  of the same  
 112 type has a vanishingly small amplitude.<sup>28</sup> Two external  
 113 microwave driving fields in the forms described above  
 114 ( $\Omega_{A,B}$ ) are applied to the qutrit, with  $\Omega_{p,q,s} \equiv \Omega$  and  
 115 three independently adjustable phases  $\phi_{p,q,s}$ . Details of  
 116 the experimental setup can be found in the Supplemental  
 117 Materials.

118 **CCI dynamics.** We first study the CCI dynamics of  
 119 the system by measuring its time evolution at different  
 120 values of  $\phi$ . Figure 2(a) shows the temporal sequence of  
 121 operations. The system is initialized in the first excited  
 122 state of  $|\psi(t=0)\rangle = |e\rangle$  by a standard  $X$  gate. A digi-  
 123 tal module containing three quantum gates is applied  
 124 to the qutrit, followed by an analog evolution driven by  
 125  $H_0$  with two control parameters: the time span and the  
 126 gauge-invariant phase  $\phi$ . Another digital module, which  
 127 is the Hermitian conjugate of the first digital module, is  
 128 applied, followed by projection measurements that yield  
 129 populations of all three states. As discussed previously,  
 130 the combined effect of the middle three blocks is to sub-  
 131 ject the system to evolve under a new Hamiltonian  $H$  as  
 132 in Eq. (2):  $e^{-iHt/\hbar} \equiv T e^{-iH_0 t/\hbar} T^\dagger$ .

133 The gauge-invariant phase  $\phi$  assumes a role as the flux  
 134 of a synthetic magnetic field, which controls the dynamic-  
 135 s of the system. At  $\phi = 0$ , the populations evolve in time  
 136 with a symmetric pattern without a preferred direction  
 137 of circulation (middle panel, Fig. 2(a)). Such symmetry  
 138 in the circulation pattern is not observed for values of  
 139  $\phi$  that are not integers of  $\pi$ . Two examples correspond-  
 140 ing to  $\phi = \pm\pi/2$  are shown in Fig. 2(a). In each case,  
 141 a circulation of certain chirality is observed: clockwise  
 142 for  $\phi = -\pi/2$  and counterclockwise for  $\phi = \pi/2$ . Such  
 143 differences are rooted in the symmetry of the system up-  
 144 on time reversal. An examination of the time-reversal  
 145 symmetry (TRS) in a strict sense requires reversing the  
 146 flow of time, which is of course not experimentally feasi-  
 147 ble. However, the periodicity presented in the evolutions  
 148 shown in Fig. 2(a) allows for a practical definition of the  
 149 TRS:  $\psi(t) = \psi(T_0 - t)$ , where  $T_0$  is the period of a given  
 150 evolution<sup>5</sup>. By comparing the evolutions from  $t = 0$  for-

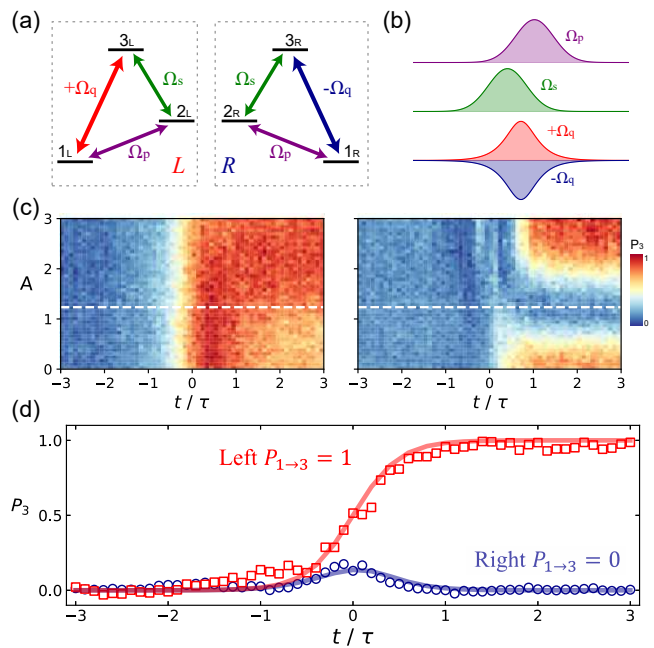


FIG. 3. Chiral separation via CCI. (a) Coupling schemes of chiral molecules with  $L$  and  $R$  handedness. Identical drivings result in a difference of  $\pi$  in the overall phase of the loop, indicated here as different couplings ( $\pm\Omega_q$ ) between the states of 1 and 3. (b) Pulse sequence for the driving fields  $\Omega_p(t)$ ,  $\Omega_s(t)$ , and  $\pm\Omega_q(t)$ . (c) Measured population  $P_3$  versus time and pulse area  $A\pi$  for  $L$  (left panel) and  $R$  (right panel) handedness, where the initial state  $|\psi_0\rangle = |1\rangle$ . The maximum population contrast is obtained when  $A \approx 1.23$  (indicated by the white dashed lines).  $t = 0$  corresponds to the moment when the  $\pm\Omega_q$  pulse reaches its maximum magnitude. (d) The population  $P_3$  as a function of time for  $A = 1.23$ , showing that the transfer to the state of 3 is nearly perfect for  $L$  handedness, but completely suppressed for  $R$  handedness.

151 ward and from  $t = T_0$  backward, Fig. 2(a) shows that the  
 152 TRS is preserved for  $\phi = 0$ , but broken for  $\phi = \pm\pi/2$ .

153 In addition to demonstrating the phase-controlled dynam-  
 154 ics under CCI, we mapped out the electronic structure of the system as a function of  $\phi$ . The eigenenergies  
 155 of  $H$  are given by  $E_k = \Omega \cos[\phi/3 - \varphi_0(k+1)]$ , with  
 156  $k \in \{1, 2, 3\}$  and  $\varphi_0 = 2\pi/3$ . A Fourier transformation  
 157 of the measured populations can reveal the energy differ-  
 158 ences  $|E_m - E_n|$  with  $m, n \in \{1, 2, 3\}$  and  $m \neq n$ , as  
 159 shown in Fig. 2(b), which agree with the simulated re-  
 160 sults using  $H$  in Eq. (2). The anti-crossings at  $\phi = \pm\pi$   
 161 in the spectrum can be explained by the slight detuning  
 162 of the coherent drives and environmental fluctuations.<sup>20</sup>

164 **Chiral separation.** Beyond constant driving fields,  
 165 we further consider a closed loop driven by three time-  
 166 dependent fields  $\Omega_p(t)$ ,  $\Omega_s(t)$ , and  $\Omega_q(t)$ , which was pro-  
 167 posed to detect and separate enantiomers with  $L$  and  $R$   
 168 handedness by using the phase-sensitive interferometric  
 169 nature of the closed-loop configuration.<sup>27</sup>

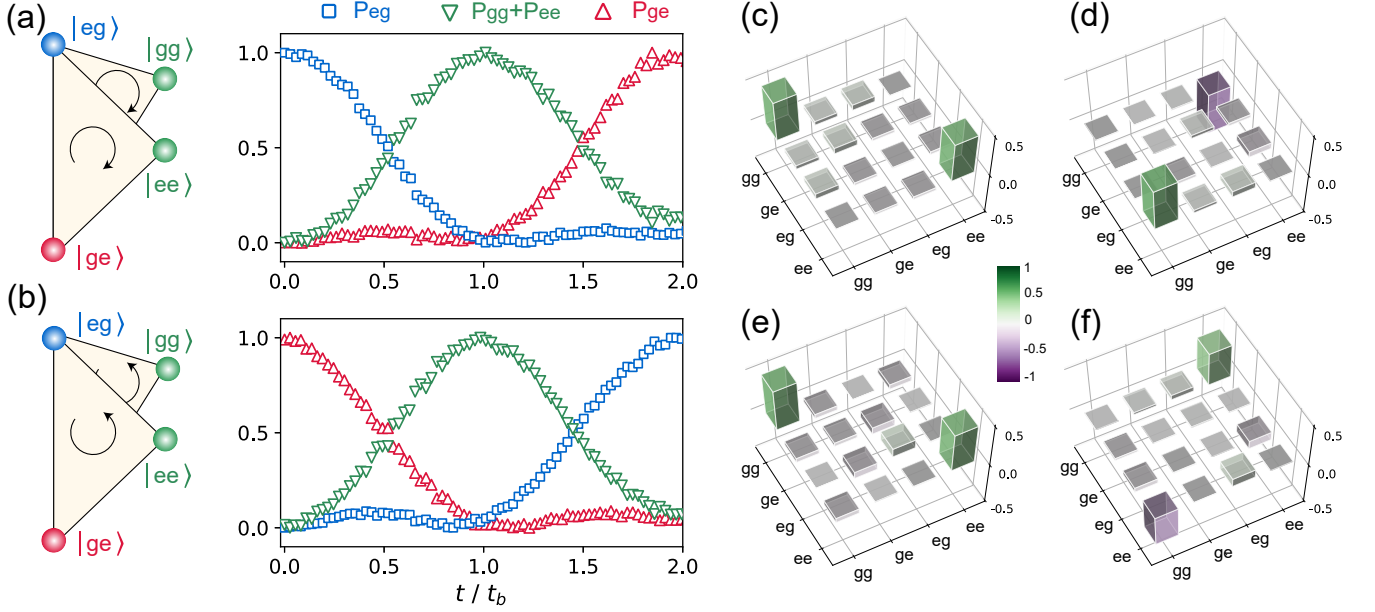


FIG. 4. Generation of entangled states using CCI. (a-b) The measured populations of  $P_{eg}$ ,  $P_{ge}$ , and  $P_{gg} + P_{ee}$ . The non-entangled states  $|eg\rangle$  and  $|ge\rangle$  in (a) and (b) evolve into the entangled states of  $(|gg\rangle \pm i|ee\rangle)/\sqrt{2}$  within time  $t_b$  under the maximum TRS breaking condition  $\phi = \pm\pi/2$ . (c) Real and (d) imaginary parts of the density matrix for the entangled state of  $(|gg\rangle + i|ee\rangle)/\sqrt{2}$ , constructed from data obtained by quantum state tomography. (e) Real and (f) imaginary parts for the state of  $(|gg\rangle - i|ee\rangle)/\sqrt{2}$ .

For a three-level system subjected to a pumping drive  $\Omega_p(t)$  ( $|1\rangle \leftrightarrow |2\rangle$ ) and Stokes drive  $\Omega_s(t)$  ( $|2\rangle \leftrightarrow |3\rangle$ ) (see Fig. 3(a); for consistency with the literature, here we label the three states as  $|1\rangle$ ,  $|2\rangle$ , and  $|3\rangle$ ), the three eigenenergies and corresponding eigenstates are  $\lambda_{\pm} = \pm\sqrt{\Omega_p^2 + \Omega_s^2}$ ,  $\lambda_0 = 0$ , and  $|\chi_{\pm}\rangle = (\sin\theta|0\rangle \pm |2\rangle + \cos\theta|3\rangle)$ ,  $|\chi_0\rangle = \cos\theta|1\rangle - \sin\theta|3\rangle$ , with  $\tan\theta(t) = \Omega_p(t)/\Omega_s(t)$ . In the celebrated technique of stimulated Raman adiabatic passage,<sup>29</sup> the two pulses are arranged in a counterintuitive order with the Stokes pulse coming first, and the eigenstate  $|\chi_0\rangle$  evolves adiabatically from  $|1\rangle$  to  $|-3\rangle$  as  $\theta$  varies from 0 to  $\pi/2$ , thus accomplishing a nearly perfect state transfer coherently.

It has been shown that by adding a counterdiabatic driving  $\Omega_q(t)$  ( $|1\rangle \leftrightarrow |3\rangle$ ) to close the loop, the resultant dynamics of the population become dependent on the handedness of the system.<sup>30,31</sup> In particular, with the same driving fields, the Hamiltonian of the system is  $H^{L,R} = (\Omega_p|2\rangle\langle 1| + \Omega_s|3\rangle\langle 2| \pm \Omega_q e^{i\phi}|3\rangle\langle 1|) + H.c.$  (Fig. 3(a)), where the  $+$ ( $-$ ) sign is for  $L$ ( $R$ ) handedness, and  $H.c.$  is the Hermitian conjugate. Such a sign difference will result in the same counterdiabatic driving doubling or canceling the nonadiabatic coupling presented in the system, depending on its handedness. If  $\phi$  is set to  $-\pi/2$ , then the populations of the final state,  $P_3$ , of the enantiomers with  $L$  and  $R$  handedness are different. For example, with carefully chosen values of the pulse areas, the handedness can be efficiently determined by

measuring  $P_3$  alone, where  $P_3 = 1$  ( $P_3 = 0$ ) for  $L$ ( $R$ ) handedness.<sup>27</sup> We note that such a counterdiabatic driving was originally proposed to accelerate various adiabatic processes, but here its major effect is to differentiate the  $L$  and  $R$  handedness.

We use pump and Stokes pulses of a Gaussian form in our experiment:  $\Omega_p(t) = \Omega_0 e^{-(t-\tau/2)^2/\tau^2}$ ,  $\Omega_s(t) = \Omega_0 e^{-(t+\tau/2)^2/\tau^2}$ . Both pulses have a width of  $\tau$  and are delayed by the same amount. A third pulse in the form of  $\Omega_q(t) = \pm 2\dot{\theta}(t)$  is applied, where the  $+$ ( $-$ ) sign corresponds to  $L$ ( $R$ ) handedness. We prepare the system in an initial state of  $|\chi_0\rangle$ . As discussed above, for  $L$  handedness, the nonadiabatic transition is canceled by  $\Omega_q(t)$  and the system remains in the state  $|\chi_0\rangle$ , inducing a perfect population transfer from  $|1\rangle$  to  $|3\rangle$  with  $P_{1\rightarrow 3} = 1$  as  $\theta(t)$  evolves from 0 to  $\pi/2$ . Conversely, for  $R$  handedness, the nonadiabatic transition doubles, which enables  $|\chi_0\rangle \rightarrow |\chi_{\pm}\rangle$  and  $P_{1\rightarrow 3} < 1$ . Figure 3(c) shows the time evolution of  $P_3$  with different pulse areas  $A\pi$ , which is defined as  $\int \Omega_{p,s} dt = \Omega_0 \tau \sqrt{\pi} \equiv A\pi$ . The driving fields  $\Omega_{p,s,q}$  in Fig. 3(b) result in a population transfer  $|1\rangle \rightarrow |3\rangle$  for  $L$  handedness with  $P_{1\rightarrow 3} = 0.986$ , and a suppression of the same transfer for  $R$  handedness with  $P_{1\rightarrow 3} = 0.003$  when  $A \approx 1.23$  (Fig. 3(d)).

**Entanglement generation with CCI.** Next, we extend the generation of CCI via pure microwave drivings to a more complex system of two coupled qubits, and

225 further demonstrate a new mechanism of entangling two  
226 qubits based on CCI, different from existing schemes that  
227 are widely used in quantum information processing with  
228 superconducting quantum circuits.

229 Consider the four-level system formed by two Xmon su-  
230 perconducting qubits with a coupling strength of  $J$  (see  
231 Fig. 1(b)). We apply two transverse resonant driving  
232 fields to the two qubits, with an identical amplitude of  
233  $J/\sqrt{2}$  and a phase difference of  $\phi_a - \phi_b = \phi$ . Similar to the  
234 single-qubit case discussed above, we combine the natu-  
235 ral evolution of such a driven system (an analog module)  
236 and a unitary operation  $T'$  (two digital modules imple-  
237 mented via standard gate operations) to realize an effec-  
238 tive Hamiltonian for a three-state system  $\{|eg\rangle, |ge\rangle, |gg\rangle\}$   
239 that can host CCI (see Fig. 1(b) and Methods). Further-  
240 more, we can generate entangled states of the two qubits  
241 by removing the unitary operation  $T'$ , since it transform-  
242 s the entangled state  $|gg\rangle + e^{i\phi}|ee\rangle$  to the ground state  
243  $|gg\rangle$ , and the special form of  $T'e^{-iHt}T'^{\dagger}$  used in this work  
244 mathematically corresponds to a linear transformation in  
245 the Hilbert space.

246 Specifically, the two-qubit system can be directly  
247 transferred from the non-entangled state  $|eg\rangle$  or  $|ge\rangle$  to  
248 the maximum entangled states of  $(|gg\rangle \pm i|ee\rangle)/\sqrt{2}$  (Fig.  
249 4(a) and (b)), within a time of  $t_b = 2\pi/(3\sqrt{3}J)$ , under  
250 the condition of maximum TRS breaking at  $\phi = \pm\pi/2$ .  
251 The density matrices  $\rho_{\pm}$  of the entangled states  $|\psi_{\pm}\rangle$   
252 characterized by quantum state tomography are given  
253 in Fig. 4(c)-(f), with fidelities of  $F_+ = 0.963 \pm 0.026$   
254 and  $F_- = 0.923 \pm 0.029$ . The analytical form of the  
255 nontrivial two-qubit unitary operator  $e^{-iHt_b}$  is given in  
256 the Supplementary Information. This new mechanis-  
257 m to generate entanglement based on chiral CCI dy-  
258 namics is different from the previous constructions of  
259 iSWAP<sup>32,33</sup> and controlled-Z gates,<sup>34-36</sup> formed by the  
260 subspace  $\{|ge\rangle, |eg\rangle\}$  or  $\{|ee\rangle, |fg\rangle\}$  in superconducting  
261 qubits.

262 **Discussion.** We have proposed and experimentally  
263 demonstrated an effective realization of CCI in genuine  
264 three-level systems that do not host CCI inherently due  
265 to certain symmetry constraints. By assembling an ana-  
266 log module of the natural evolution governed by their o-  
267 riginal Hamiltonians with carefully designed digital mod-  
268 ules, we can effectively bypass such constraints and es-  
269 tablish a CCI without auxiliary driving signals that are  
270 technically challenging to implement. Based on such a  
271 CCI, we can demonstrate a variety of interesting related  
272 phenomena such as a phase-controlled chiral dynamic-  
273 s, chiral separation, and a new mechanism to generate  
274 entangled states.

275 The hybrid digital-analog approach used here is es-  
276 sential to our work, since on the one hand the above  
277 symmetry constraints forbid an inherent CCI that would  
278 manifest in the analog evolutions of the systems, and on  
279 the other hand, a pure digital approach is practically in-

280 feasible, as too many quantum gate operations would be  
281 required, especially to simulate the natural evolutions of  
282 the systems. This work serves as a preliminary demon-  
283 stration of the enriched possibilities for quantum simu-  
284 lation by the hybrid digital-analog approach. One can  
285 reasonably expect, by assembling more sophisticated and  
286 ingeniously engineered analog and digital modules, the  
287 realm of quantum simulation that is accessible by pure  
288 analog or digital approaches can be largely expanded, a  
289 welcome development before we realize a universal and  
290 fault-tolerant digital quantum computer.

## 291 Methods

292 **Experimental setup.** We used the Xmon-type of superconduct-  
293 ing qutrit with a tunable frequency via a bias current on a Z-control  
294 line. Microwave pulses are applied to the qutrit via an XY-control  
295 line. The state of the qutrit can be deduced by measuring the  
296 transmission coefficient  $S_{21}$  of the transmission line using a stan-  
297 dard dispersive measurement<sup>37</sup>. For the part of experiment involv-  
298 ing two qubits, they are coupled via an ancillary qubit that can fine  
299 tune the effective coupling strength<sup>38</sup>. Further details of the sam-  
300 ples and measurement setup can be found in the Supplementary  
301 Information.

302 **Effective Hamiltonian of the three-level system.** The ef-  
303 fective Hamiltonian of the microwave-driven qutrit in a rotat-  
304 ing frame described by the operator  $U = |g\rangle\langle g| + |e\rangle\langle e|e^{i\omega_A t} +$   
305  $|f\rangle\langle f|e^{i(\omega_A t + \omega_B t)}$  and under the rotating-wave approximation is  
306 given by Eq. 1. The unitary operator  $T$  that serves as a digital  
307 module is

$$T = \begin{pmatrix} 1/\sqrt{2} & 0 & -e^{i\phi_q}/\sqrt{2} \\ 0 & 1 & 0 \\ e^{-i\phi_q}/\sqrt{2} & 0 & 1/\sqrt{2} \end{pmatrix}, \quad (3)$$

309 which can be constructed from three single-qutrit gates  $R_{e,f}(\pi, 0) \cdot$   
310  $R_{g,e}(\pi/2, -\phi_q) \cdot R_{e,f}(\pi, \pi)$ , where  $R_{m,n}(\theta, \phi)$  represents a rotation  
311 in the subspace of  $\{|m\rangle, |n\rangle\}$ :

$$R_{m,n}(\theta, \phi) = \begin{pmatrix} \cos(\theta/2) & -e^{-i\phi} \sin(\theta/2) \\ e^{i\phi} \sin(\theta/2) & \cos(\theta/2) \end{pmatrix}. \quad (4)$$

312 The combination of the natural evolution of the original Hamil-  
313 tonian and the unitary operations gives the effective Hamiltonian  $H$   
314 in Eq. (2):  $e^{-iHt/\hbar} \equiv T e^{-iH_0 t/\hbar} T^{\dagger}$ , which describes a three-level  
315 system with CCI.

316 **Effective Hamiltonian of the four-level system.** Consid-  
317 er the four-level system formed by two coupled superconducting  
318 qubits with a coupling strength of  $J$ . We apply two transverse  
319 resonant driving fields, one to each qubit, with identical frequency  
320  $\omega_a = \omega_b = \omega_{ge}$  and amplitude  $|\Omega_A| = |\Omega_B| = J/\sqrt{2}$ , and a phase  
321 difference of  $\phi_a - \phi_b = \phi$ . In a rotating frame described by an op-  
322 erator  $U = (|g\rangle\langle g| + |e\rangle\langle e|e^{i\omega_a t}) \otimes (|g\rangle\langle g| + |e\rangle\langle e|e^{i\omega_b t})$  and under  
323 the rotating-wave approximation, the Hamiltonian is given by

$$H/\hbar = J(\cos\phi\sigma_x^a + \sin\phi\sigma_y^a + \sigma_x^b)/\sqrt{2} + J(\sigma_x^a \otimes \sigma_x^b + \sigma_y^a \otimes \sigma_y^b)/2$$

$$= \frac{J}{\sqrt{2}} \begin{pmatrix} 0 & 1 & e^{-i\phi} & 0 \\ 1 & 0 & \sqrt{2} & e^{-i\phi} \\ e^{i\phi} & \sqrt{2} & 0 & 1 \\ 0 & e^{i\phi} & 1 & 0 \end{pmatrix}. \quad (5)$$

324 Combining the natural evolution governed by this Hamiltonian and  
325 a unitary operation defined as

$$T' = \frac{1}{\sqrt{2}} \begin{pmatrix} 1 & 0 & 0 & e^{-i\phi} \\ 0 & \sqrt{2} & 0 & 0 \\ 0 & 0 & \sqrt{2} & 0 \\ -e^{i\phi} & 0 & 0 & 1 \end{pmatrix} \quad (6)$$

326 gives an effective Hamiltonian  $H'$  via  $e^{-iH't/\hbar} \equiv T'e^{-iHt/\hbar}T'^{\dagger}$ :

$$H' = J \left( |eg\rangle\langle ge| + |ge\rangle\langle gg| + e^{i\phi}|eg\rangle\langle gg| + H.c. \right). \quad (7)$$

327 This new Hamiltonian describes a three-level system with CCI. If  
328 the two unitary operations,  $T'$  and  $T'^{\dagger}$  are dropped, then Eq. (7)  
329 becomes

$$\bar{H}' = J \left( |\bar{1}\rangle\langle\bar{2}| + |\bar{2}\rangle\langle\bar{3}| + e^{i\phi}|\bar{1}\rangle\langle\bar{3}| + H.c. \right). \quad (8)$$

330 Here,  $\{|\bar{1}\rangle, |\bar{2}\rangle, |\bar{3}\rangle\}$  form an invariant triplet subspace  
331 of the overall Hilbert space of  $\{|\bar{1}\rangle, |\bar{2}\rangle, |\bar{3}\rangle, |\bar{D}\rangle\} \equiv$   
332  $\{|eg\rangle, |ge\rangle, (|gg\rangle + e^{i\phi}|ee\rangle)/\sqrt{2}, (|gg\rangle - e^{i\phi}|ee\rangle)/\sqrt{2}\}$ , and  
333 the state of  $|D\rangle$  is a dark state that is decoupled from the system  
334 evolution.

\* Z. T. and L. Z. contributed equally to this work.

† lius3@sustech.edu.cn

‡ yantx@sustech.edu.cn

§ chenyz@sustech.edu.cn

- [1] I. M. Georgescu, S. Ashhab, and F. Nori, *Rev. Mod. Phys.* **86**, 153 (2014).
- [2] R. Barends, L. Lamata, J. Kelly, L. Garcia-Ivarez, A. G. Fowler, A. Megrant, E. Jeffrey, T. C. White, D. Sank, J. Y. Mutus, B. Campbell, Y. Chen, Z. Chen, B. Chiaro, A. Dunsworth, I.-C. Hoi, C. Neill, P. J. J. O'Malley, C. Quintana, P. Roushan, A. Vainsencher, J. Wenner, E. Solano, and J. M. Martinis, *Nat. Commun.* **6**, 7654 (2015).
- [3] R. Barends, A. Shabani, L. Lamata, J. Kelly, A. Mezzacapo, U. L. Heras, R. Babbush, A. G. Fowler, B. Campbell, Y. Chen, Z. Chen, B. Chiaro, A. Dunsworth, E. Jeffrey, E. Lucero, A. Megrant, J. Y. Mutus, M. Neeley, C. Neill, P. J. J. O'Malley, C. Quintana, P. Roushan, D. Sank, A. Vainsencher, J. Wenner, T. C. White, E. Solano, H. Neven, and J. M. Martinis, *Nature* **534**, 222 (2016).
- [4] S. Lloyd, *Science* **273**, 1073 (1996).
- [5] P. Roushan, C. Neill, A. Megrant, Y. Chen, R. Babbush, R. Barends, B. Campbell, Z. Chen, B. Chiaro, and A. D. et al., *Nat. Phys.* **13**, 146 (2016).
- [6] D. W. Wang, C. Song, W. Feng, H. Cai, D. Xu, H. Deng, H. Li, D. Zheng, X. Zhu, H. Wang, S. Y. Zhu, and M. O. Scully, *Nat. Phys.* **15**, 382 (2019).
- [7] W. Cai, J. Han, F. Mei, Y. Xu, Y. Ma, X. Li, H. Wang, Y. P. Song, Z.-Y. Xue, Z.-q. Yin, S. Jia, and L. Sun, *Phys. Rev. Lett.* **123**, 080501 (2019).
- [8] W. Liu, W. Feng, W. Ren, D.-W. Wang, and H. Wang, *Appl. Phys. Lett.* **116**, 114001 (2020).
- [9] A. Mezzacapo, U. L. Heras, J. S. Pedernales, L. DiCarlo, E. Solano, and L. Lamata, *Sci. Rep.* **4**, 7482 (2015).
- [10] L. Lamata, *Sci. Rep.* **7**, 43768 (2017).
- [11] L. Lamata, A. Parra-Rodriguez, M. Sanz, and E. Solano, *Advances in Physics: X* **3**, 1457981 (2018).
- [12] A. Parra-Rodriguez, P. Lougovski, L. Lamata, E. Solano, and M. Sanz, *Phys. Rev. A* **101**, 022305 (2020).
- [13] I. I. Rabi, *Phys. Rev.* **49**, 324 (1936).
- [14] N. K. Langford, R. Sagastizabal, M. Kounalakis, C. Dickel, A. Bruno, F. Luthi, D. J. Thoen, A. Endo, and L. DiCarlo, *Nat. Commun.* **8**, 1715 (2017).
- [15] D. F. Phillips, A. Fleischhauer, A. Mair, R. L. Walsworth, and M. D. Lukin, *Phys. Rev. Lett.* **86**, 783 (2001).
- [16] J. Vanier, *Appl. Phys. B* **81**, 421 (2005).
- [17] J. I. Cirac, P. Zoller, H. J. Kimble, and H. Mabuchi, *Phys. Rev. Lett.* **78**, 3221 (1997).
- [18] D. V. Kosachiov, B. G. Matisov, and Y. V. Rozhdestvensky, *J. Phys. B: At., Mol. Opt. Phys.* **25**, 2473 (1992).
- [19] S. J. Buckle, S. M. Barnett, P. L. Knight, M. A. Lauder, D. T. Pegg, and D. T. Pegg, *Opt. Acta* **33**, 1129 (1986).
- [20] A. Barfuss, J. Klbl, L. Thiel, J. Teissier, M. Kasperczyk, and P. Maletinsky, *Nat. Phys.* **14**, 1087 (2018).
- [21] P. Král and M. Shapiro, *Phys. Rev. Lett.* **87**, 183002 (2001).
- [22] P. Král, I. Thanopoulos, M. Shapiro, and D. Cohen, *Phys. Rev. Lett.* **90**, 033001 (2003).
- [23] C. Ye, Q. Zhang, and Y. Li, *Phys. Rev. A* **98**, 063401 (2018).
- [24] W. S. Knowles, *Angew. Chem., Int. Ed. Engl.* **41**, 1998 (2002).
- [25] A. Vepsäläinen, S. Danilin, and G. Sorin Paraoanu, *Sci. Adv.* **5**, 5999 (2019).
- [26] A. Vepsäläinen and G. S. Paraoanu, *Adv. Quantum Technol.* **2020**, 1900121 (2020).
- [27] N. V. Vitanov and M. Drewsen, *Phys. Rev. Lett.* **122**, 173202 (2019).
- [28] J. Koch, T. M. Yu, J. Gambetta, A. A. Houck, D. I. Schuster, J. Majer, A. Blais, M. H. Devoret, S. M. Girvin, and R. J. Schoelkopf, *Phys. Rev. A* **76**, 1 (2007).
- [29] N. V. Vitanov, A. A. Rangelov, B. W. Shore, and K. Bergmann, *Rev. Mod. Phys.* **89**, 015006 (2017).
- [30] X. Chen, I. Lizuain, A. Ruschhaupt, D. Guéry-Odelin, and J. G. Muga, *Phys. Rev. Lett.* **105**, 123003 (2010).
- [31] D. Guéry-Odelin, A. Ruschhaupt, A. Kiely, E. Torrontegui, S. Martínez-Garaot, and J. G. Muga, *Rev. Mod. Phys.* **91**, 045001 (2019).
- [32] N. Schuch and J. Siewert, *Phys. Rev. A* **67**, 032301 (2003).
- [33] R. C. Bialczak, M. Ansmann, M. Hofheinz, E. Lucero, M. Neeley, A. D. O'Connell, D. Sank, H. Wang, J. Wenner, M. Steffen, A. N. Cleland, and J. M. Martinis, *Nat. Phys.* **6**, 409 (2010).
- [34] F. W. Strauch, P. R. Johnson, A. J. Dragt, C. J. Lobb, J. R. Anderson, and F. C. Wellstood, *Phys. Rev. Lett.* **91**, 167005 (2003).
- [35] T. Yamamoto, M. Neeley, E. Lucero, R. C. Bialczak, J. Kelly, M. Lenander, M. Mariani, A. D. O'Connell, D. Sank, H. Wang, M. Weides, J. Wenner, Y. Yin, A. N. Cleland, and J. M. Martinis, *Phys. Rev. B* **82**, 184515 (2010).
- [36] J. Ghosh, A. Galiautdinov, Z. Zhou, A. N. Korotkov, J. M. Martinis, and M. R. Geller, *Phys. Rev. A* **87**, 022309 (2013).
- [37] A. Wallraff, D. I. Schuster, A. Blais, L. Frunzio, J. Majer, M. H. Devoret, S. M. Girvin, and R. J. Schoelkopf, *Phys. Rev. Lett.* **95**, 060501 (2005).
- [38] F. Yan, P. Krantz, Y. Sung, M. Kjaergaard, D. L. Campbell, T. P. Orlando, S. Gustavsson, and W. D. Oliver, *Phys. Rev. Appl.* **10**, 054062 (2018).

### Acknowledgements

This work was supported by the Key-Area Research and Development Program of Guang-Dong Province (Grant No. 2018B030326001), the National Natural Science Foundation of China (U1801661), the Guangdong Innovative and Entrepreneurial Research Team Program

444 (2016ZT06D348), the Guangdong Provincial Key Labo-  
445 ratory (Grant No.2019B121203002), the Natural Science  
446 Foundation of Guangdong Province (2017B030308003),  
447 and the Science, Technology and Innovation Commission  
448 of Shenzhen Municipality (JCYJ20170412152620376,  
449 KYTDPT20181011104202253).

#### 450 **Author contributions**

451 Z. T. and L. Z. contributed equally to this work. T. Y. and  
452 Z. T. conceived the experiment; Z. T. designed the theoret-  
453 ical protocol and performed the experiment with T. Y. under  
454 the supervision of Y. C.; L. Z. designed the superconducting  
455 devices used in the experiment, and fabricated them togeth-  
456 er with Y. Z. and H. J.; T. Y., Z. T., and Y. C. wrote the  
457 manuscript together, with inputs from all authors.

# Figures

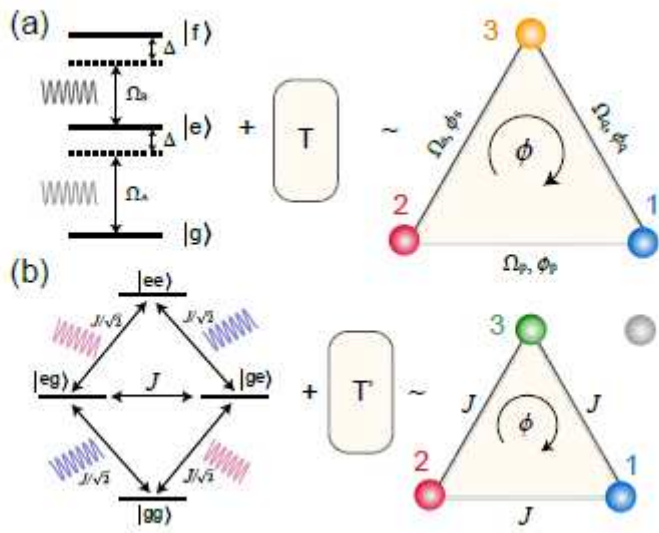


Figure 1

Realization of CCI with a hybrid digital-analog approach.

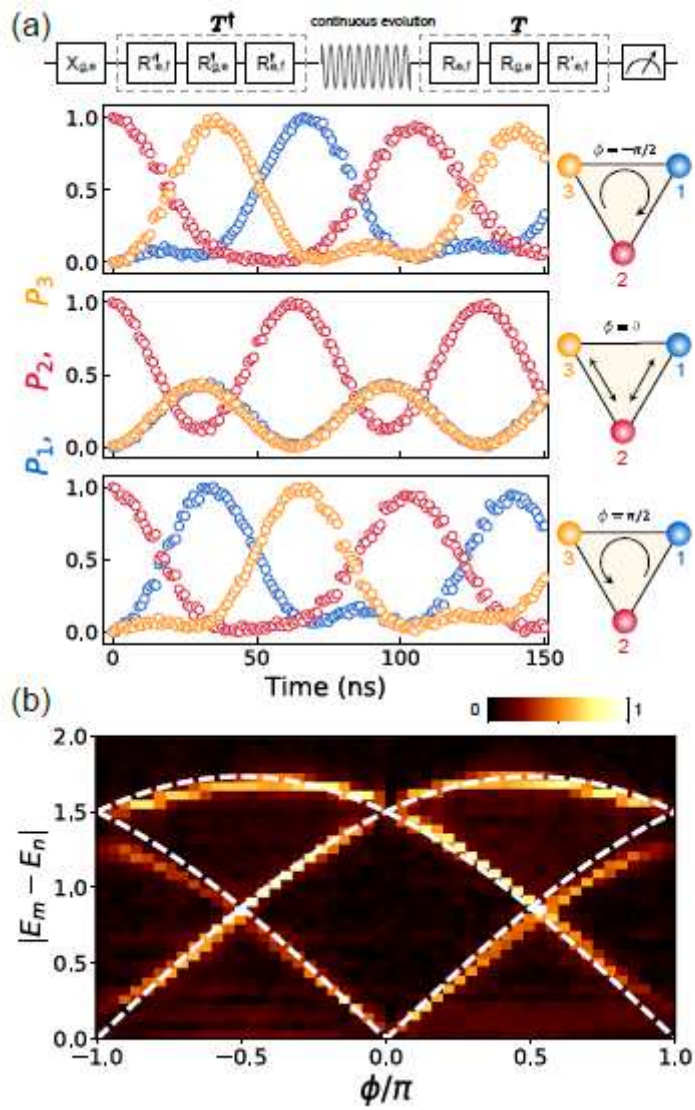


Figure 2

Phase-controlled quantum dynamics resulting from CCI in a single qutrit (see Fig. 1(a)).

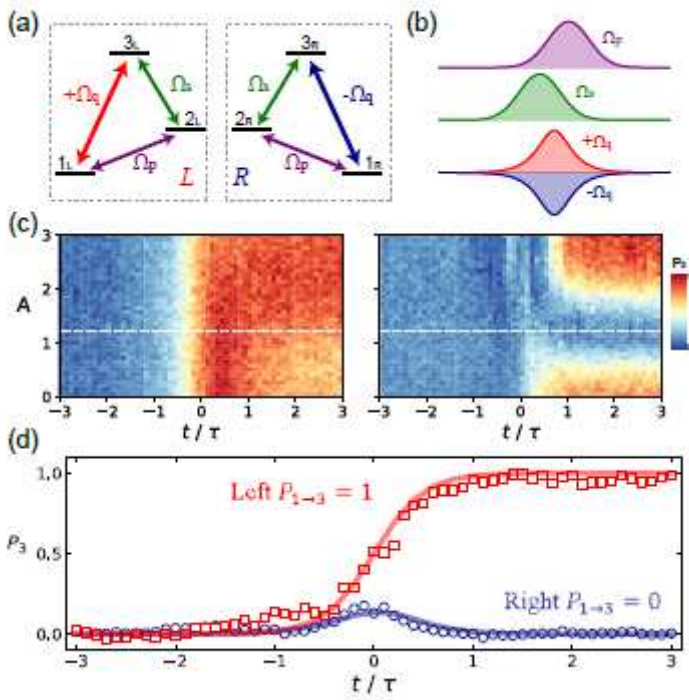


Figure 3

Chiral separation via CCI.

4

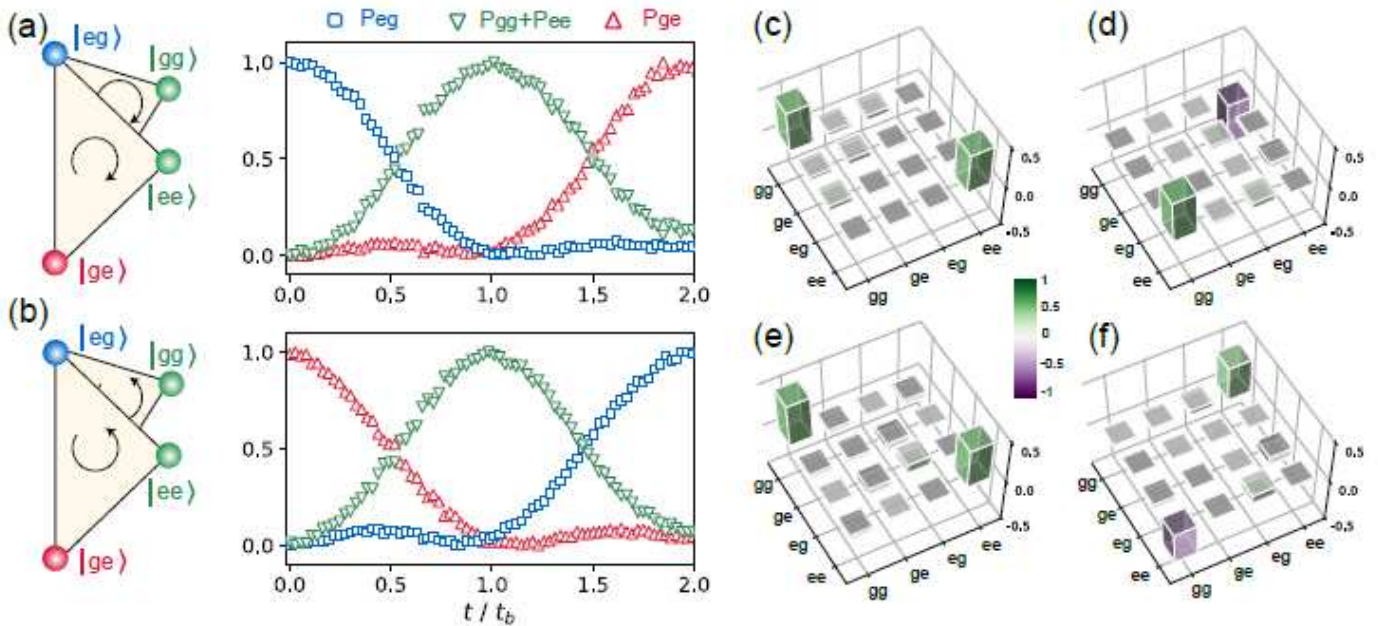


Figure 4

Generation of entangled states using CCI.

## Supplementary Files

This is a list of supplementary files associated with this preprint. Click to download.

- [supplyCCI.pdf](#)
- [NCsupply.pdf](#)